

# Radiometric Studies and Base Line Calibrations for NORM and TENORM Studies

Debashish Sengupta, Saurabh Mittal and Kajori Parial

**Abstract** Natural ambient radiations are present everywhere due to the spontaneous emissions by radioactive elements. There are two sources of radiations in the earth's environment: cosmic and terrestrial. Cosmic radiation originates from high-energy cosmic ray particle interaction with the Earth's atmosphere, and terrestrial radiation comes from the naturally occurring radioactive materials (NORM) present in the Earth's crust. Radiometric studies provide a suitable tool for detecting and measuring the natural radiation. Radioactivity measurements are also referred to as baseline measurements when the radioactivity is only from NORM. Baseline measurements provide the background measurements for comparative studies, since background radiation is not the same everywhere. There are some regions in the world with higher levels of radiation, known as high background radiation areas (HBRAs); a few places even have much higher background radiation, and are known as very high background radiation areas (VHBRAs). In this chapter, applications of radioactivity measurements are demonstrated with case studies for various studies, namely characterization of the area as background or HBRAs or VHBRAs, environmental studies for assessing the hazard due to radiation and locating hot springs. Mining and production of uranium also cause environmental radioactivity, termed as technologically enhanced naturally occurring radioactive material (TENORM). Radiometric studies also provide classification of activity under NORM and TENORM. Some of the recent studies undertaken primarily by us in this regard are discussed along with their implications.

The studies presented in the Chapter reflect the significance of research related to integrated near-surface geophysics for various applications, namely radiometric measurements, contamination studies primarily due to anthropogenic causes, shallow subsurface exploration for economic deposits like shale gas, coal bed methane, and associated rare earths.

**Keywords** NORM and TENORM · Near surface geophysics · High background radiation areas (HBRAs) · Radioactivity measurements · Uranium exploration

---

D. Sengupta (✉) · S. Mittal · K. Parial  
Department of Geology and Geophysics, Indian Institute of Technology Kharagpur,  
Kharagpur, West Bengal 721302, India  
e-mail: dsagg@gg.iitkgp.ernet.in

D. Sengupta (ed.), *Recent Trends in Modelling of Environmental Contaminants*,  
DOI 10.1007/978-81-322-1783-1\_1, © Springer India 2014

## 1 Introduction

Naturally occurring radionuclides are present all over the Earth's crust in varying quantities depending on the ambient geological and geochemical environment. The considerable concentration of radionuclides in soil, water, air, and living organisms is due to the presence of naturally occurring radioactive elements like  $^{232}\text{Th}$ ,  $^{238}\text{U}$ , and  $^{40}\text{K}$  that occur mostly in minerals such as monazite and zircon. The reason for their presence today since the origin of Earth is their sufficiently long half-lives. Their half-lives are comparable to the age of the Earth and therefore these are called primordial radionuclides. The major contribution to environmental radiation is from  $^{232}\text{Th}$ ,  $^{238}\text{U}$ ,  $^{40}\text{K}$  and their decay products; other radionuclides, namely  $^{235}\text{U}$ ,  $^{87}\text{Rb}$ ,  $^{138}\text{La}$ ,  $^{147}\text{Sm}$ , etc. also exist in nature but in such low quantities that their contribution to the ambient environmental radiation can be neglected.

Natural radiation, also known as ambient radiation or background radiation, is quantified by the natural radiation environment. There are two sources of background radiation in the environment: cosmic and terrestrial. Cosmic radiation originates from high-energy cosmic ray particle interaction with the Earth's atmosphere. Terrestrial radiation comes from the naturally occurring radioactive materials (NORM) present in the Earth's crust. NORM include primordial radionuclides that are naturally present in the rocks and minerals of the earth's crust and cosmogenic radionuclides produced by interactions of cosmic nucleons with target atoms in the atmosphere and in the earth. NORM does not include natural radioactive material from anthropogenic sources, such as those produced by nuclear power and used in nuclear medicine. Therefore radioactive materials can be classified into (a) man-made and (b) NORM. Man-made radionuclides include Cobalt-60, Strontium-90, and Cesium-137, which are produced in nuclear reactors by nuclear fusion or nuclear fission.

TENORM is an acronym used for technologically enhanced NORM, and is produced when naturally occurring radionuclides are concentrated or their activities and exposure is increased compared with the unaltered situation by anthropogenic activities.

Terrestrial radiation affects us both internally and externally. External exposures primarily include gamma radiation. Internal radiation exposure is due to intake of radionuclides by inhalation or ingestion. The important contributor in internal exposure is radon (from uranium decay series) and its decay products. Therefore, the total exposure to radiation comes from gamma radiation (32.2%) and inhalation of radon (51.9%) (UNSCEAR 2000). Figure 1a and b shows the schematic of a radiation counter operating to detect radiation from an area of  $2\pi$  and  $>2\pi$ , respectively.

Radiometric studies coupled with other geophysical techniques provide a valuable tool for detecting and measuring the natural radiation. This also helps in the baseline calibration for the average radiation background. Table 1 represents an outline of the geophysical techniques and the attributes or parameters measured through it that can be applied along with radiometric studies for a better understanding of the ambient geology. Radioactivity measurements are also called baseline measurements when the radioactivity is from NORM and not from any other

**Fig. 1** Schematic of radiation detection. **a** Within a solid angle  $2\pi$ . **b** Within solid angle  $>2\pi$

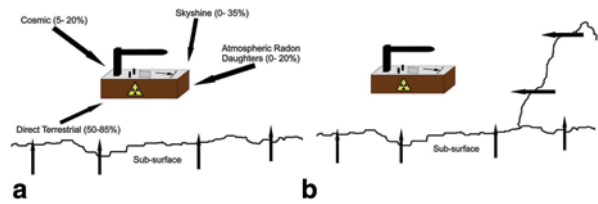


**Table 1** Geophysical techniques employed and corresponding attributes or parameters measured to identify various geological features

Relevant aspects	Geophysical methods	Output
Resistivity/Conductivity anomaly	Resistivity, VLF-EM	Faults and fractures
High or low conductivity	Resistivity, VLF-EM, radiometrics	Alteration
High conductivity, potassium content	VLF-EM, radiometrics	Hydrothermal alteration
High conductivity contrast, potassium content	VLF-EM, radiometrics	Silicification (dyke-like feature)
Weak conductor, low and patchy mineralization	Resistivity, VLF-EM	Disseminated deposit
High over low conductivity	Resistivity, VLF-EM, radiometrics	Weathering

source or by any kind of anthropogenic activity (such as mining and oil and gas production). Baseline measurements aid in the identification and quantification of naturally occurring radionuclides. It also provides the background measurements for comparative studies, since background radiation is not the same everywhere. There are some regions in the world that have higher levels of radiation, known as high background radiation areas (HBRAs). A few places in the world have an even greater level of background radiation, and are known as very high background radiation areas (VHBRAs). VHBRAs include: Guarapari, in the coastal region of Espirito Santo, Brazil (Cullen 1977; UNSCEAR 1993); Yangjiang, China (Wei et al. 1993; Wei and Sugahara 2000); the southwest coast of India (Sunta et al. 1982; Paul et al. 1998); Ramsar and Mahallat, Iran (Sohrabi 1993; Ghiassi-nejad et al. 2002); and places in some other countries (UNSCEAR 2000). Sources of background radiation include radon, monazite sand deposits, and radium. The eastern coast of Orissa, India has also been delineated as an HBRA (Mohanty et al. 2004a, b). Further details of the same have been incorporated as a case study subsequently.

Apart from characterization of the area as background or HBRA or VHBRAs, radiometric studies are helpful in environmental studies for assessing the hazard due to radiation and locating hot springs. Mining and production of uranium also cause environmental radioactivity. Such radioactivity is caused by materials formed due to anthropogenic activities like mining and oil and gas production and is termed TENORM. Baseline measurement of natural radioactivity helps in the classification of activity under NORM or TENORM. A case study explaining the migration of radon from a uranium tailing pond is also presented in this chapter.

Besides this, radiometric studies are particularly useful in the exploration of radioactive mineral deposits. An integrated geophysical survey with radiometric surveys is quite useful in providing details about the presence or absence of radioactive minerals, geometry, and the lateral extent of ore bodies. The case study provided in this chapter illustrates the advantage of radiometric studies in exploration. Radiometric data were correlated with very low frequency (VLF) electromagnetic (EM) data to investigate the possibility of shallow economic uranium deposit along the South Purulia Shear Zone (SPSZ).

The present study amply reflects the significance of research related to integrated near-surface geophysics for various applications, right from radiometric measurements and contamination studies to shallow-depth subsurface exploration for non-radioactive minerals like shale gas, coal bed methane, etc.

## ***1.1 Ionization Chambers***

### **Geiger–Müller (GM) counters**

A Geiger–Müller (GM) counter is a gas-filled cylindrical tube (cathode) with a thin metal wire (anode) (Fig. 2). When a  $\gamma$ -ray photon interacts with the wall of the cylinder an energetic electron is produced that enters the tube and ionizes the gas, creating an avalanche of electrons that moves towards the central wire. Due to high voltage within the tube a strong electric field is produced within the tube. The electrons move towards the positive electrode and the positive atoms move towards the negative electrode. A current pulse is generated as a result of this and is measured as a count. Once detected or counted the ions become neutral, restoring the GM counter to normal state, ready for count detection. The operation and efficiency of a GM counter are highly dependent on the operating voltage. Lower voltages will not record any pulse and higher voltages result in constant discharge, resulting in erroneous count. The operating voltage of a GM counter is to be strictly maintained in order to ensure maximum efficiency and the health of the detector. The simple yet efficient counting capability of GM counters makes it a reliable, cost-effective, and portable instrument for detecting total environmental radiation counts. It is mostly used for ground reconnaissance survey for identifying radioactive zones.

### **Scintillation Counters**

Scintillation counters are made up of a luminescent material connected to a device, mostly a photomultiplier tube (PMT), which detects the  $\gamma$ -ray-induced photon emission. When the incident  $\gamma$ -ray interacts with the scintillator the ionized atoms emits a photon of light to attain a lower energy level. This light energy is detected and amplified by the photo multiplier tube.

The amount of scintillation produced is proportional to the  $\gamma$ -ray energy as the entire energy is used to excite the atom. An electric pulse is generated by the PMT

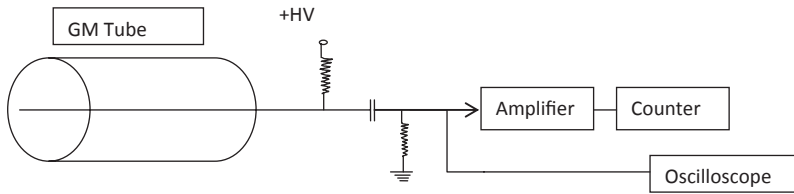


Fig. 2 Schematic diagram of Geiger–Müller (GM) counter (After Smith and Lucas 1991)

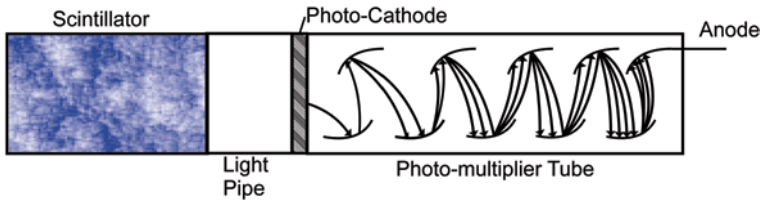


Fig. 3 Schematic diagram of Scintillation counter (After Smith and Lucas 1991)

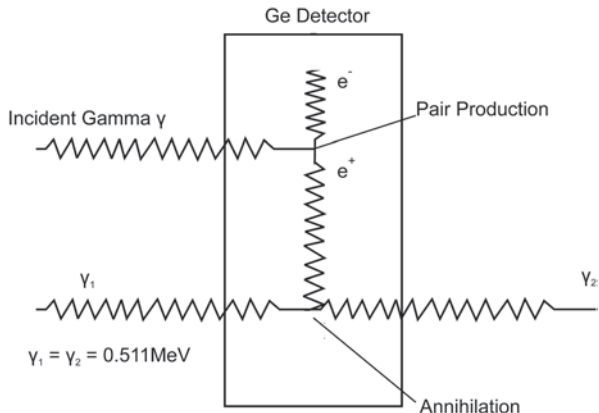
proportional to the amount the scintillation and the pulse height correlates with the incident  $\gamma$ -radiation energy. The scintillation detectors can be either organic (anthracene, plastics, etc.) or inorganic (NaI(Tl), BGO, ZnS, etc.). The scintillation counters are advantageous compared to the GM counters in terms of efficiency; however, they costlier than GM counters and are not portable enough for ground survey.

## 1.2 $\gamma$ -Ray Spectroscopy:

$\gamma$ -rays are detected based on their interaction with the charged electrons of atoms of matter. During ionization the  $\gamma$ -ray photon gives part or the whole of its energy to the electron. These electrons in turn collide with other electrons and release more electrons. The charge can be collected through GM counters (as mentioned earlier) or through the solid-state detectors. Natural radioactive sources yields a complex spectrum in contrast with mono energetic sources. The energy of the photopeak is considered to be equal to the incident  $\gamma$ -ray. Germanium (Ge) is found to be the most efficient element for solid-state semiconductor detectors. Initially, lithium-drafted Ge was used as a detector element. However, in recent times very high purity Ge is used as the detector material.

When  $\gamma$ -ray is incident on the Ge crystal an electron–hole pair is created that helps in detecting the  $\gamma$ -radiation energy. When the  $\gamma$ -ray is incident on the detector with energy greater than the band-gap energy, an electron–hole pair is created. These electrons allow the conduction of electricity, generating an electric pulse. The greater the incident energy of the  $\gamma$ -photon, the greater the pair production, thus

**Fig. 4** Process of pair production (After Khandaker 2011)



generating a higher pulse. Figure 4 shows a schematic view of the pair production generation.

The activity (in Bq/Kg) of each radionuclide in the samples is determined using the total net counts under the selected photo-peaks after subtracting the background counts, and applying factor for photo-peak efficiency  $\gamma$ -intensity of the radionuclide, the weight of the sample and the time of counting. The relationship or the formula used to calculate activity concentration is given by

$$A = (\text{dps}/w) \times 1000 \tag{1}$$

Where, A=activity concentration (in Bq/kg),  
 w=weight of the sample (in g), and  
 dps=disintegrations per second

$$\text{dps} = P / (t \times \epsilon \times I) \tag{2}$$

Here, P=net peak area,  
 t=time for which counting is done (second)  
 $\epsilon$ =efficiency of photo-peak, and  
 I= $\gamma$ -intensity of a particular radionuclide

## 2 Case Studies

### 2.1 Erasama Beach, Orissa, India (HBRA)

Terrestrial background radiation from naturally occurring radionuclides like  $^{238}\text{U}$ ,  $^{232}\text{Th}$ , and  $^{40}\text{K}$ , is a major contributor towards humankind’s exposure to radiation (UNSCEAR 2000). However, there are certain local geological factors that enhance

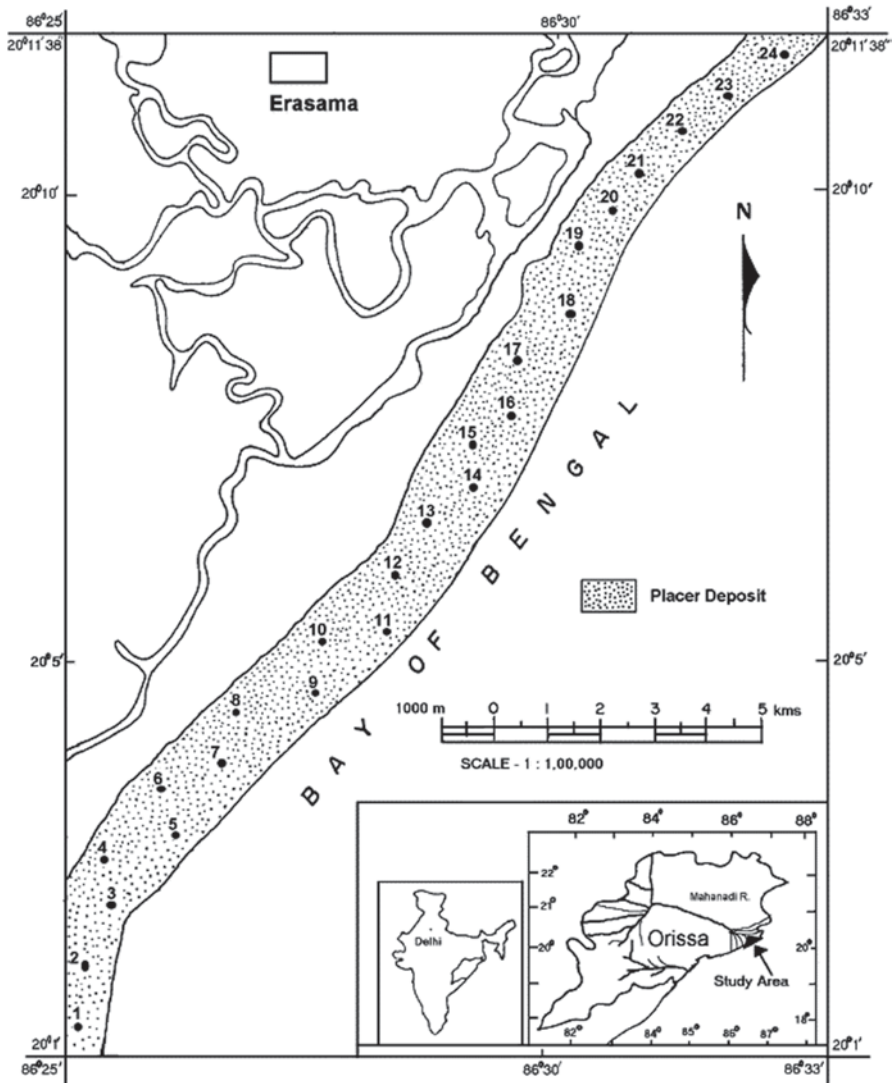


Fig. 5 Map showing Erasama beach (After Mohanty et al. 2004a)

this radiation significantly above normal (or background); these regions are known as HBRAs. In India, the Erasama beach region, on the eastern coast of Orissa, is one such HBRA. Erasama beach is a coastal strip (Lat. 86°25'–86°33'N, Long. 20°1'–20°11'E) on the eastern coast of Orissa state, India (Fig. 5). The area of study considered by Mohanty et al. (2004a) is a flat terrain with a gentle slope towards the Bay of Bengal, and consists of recent alluvium and coastal deltaic plain sediments. Extensive radiometric studies were carried by Mohanty et al. (2004a) out in

this region to measure the ambient radiation in terms of activity concentration of radionuclides.

### Radiometric Analysis

Standard procedure was followed for sampling in the field and sample preparation in the laboratory. 24 bulk sand samples and different individual fraction of mineral sands were subjected to radiometric analysis. Individual mineral fractions were separated and only zircon, sillimanite, and rutile fractions were considered for this study. Samples were dried and sealed for some time for attaining secular equilibrium between  $^{232}\text{Th}$ ,  $^{238}\text{U}$ , and their daughter products. The activity of the samples was then analysed using  $\gamma$ -ray spectrometric analysis. It was carried out at the Radiochemistry Division, Variable Energy Cyclotron Centre, BARC, Kolkata, using a coaxial HPGe detector (EG & G, ORTEC) with 15% relative efficiency.  $^{152}\text{Eu}$  liquid source (Amersham Company, UK) of known activity was used to determine the efficiency of detector, since  $^{152}\text{Eu}$  has large range of energies (122–1,408 keV) with emission abundances of 3–29% (Firestone and Shirley 1998; Grigorescu et al. 2002).

In the absence of any interference,  $^{40}\text{K}$  is measured directly by its own  $\gamma$ -rays;  $^{232}\text{Th}$  and  $^{238}\text{U}$  are indirectly measured from the  $\gamma$ -rays of their decay products. Decay products for  $^{238}\text{U}$  ( $^{214}\text{Pb}$ : 295 and 352 keV; and  $^{214}\text{Bi}$ : 609 keV) and  $^{232}\text{Th}$  ( $^{228}\text{Ac}$ : 209, 338, and 911 keV;  $^{212}\text{Pb}$ : 239 keV;  $^{212}\text{Bi}$ : 727 keV; and  $^{208}\text{Tl}$ : 583 keV) were used with the assumption that the decay series is in secular equilibrium. Mass of the sample, branching ratio of the  $\gamma$ -decay, time of counting, and efficiency of the detector were duly considered during estimation of activity concentration. After calculation of activity concentration from intensity of several  $\gamma$ -rays, they were grouped together to compute a weighted average activity per nuclide. Absorbed gamma dose rates were also calculated based on the guidelines of UNSCEAR (1993, 2000).

### Results and Discussion

A total of 24 samples were analysed. Activity concentration of  $^{232}\text{Th}$  ranged from 900–4,700  $\text{Bq kg}^{-1}$  with an average of  $2,825 \pm 50 \text{ Bq kg}^{-1}$ . However,  $^{238}\text{U}$  activity concentration ranged from 150–500  $\text{Bq kg}^{-1}$ , with an average of  $350 \pm 20 \text{ Bq kg}^{-1}$  and that of  $^{40}\text{K}$  ranged from 100–250  $\text{Bq kg}^{-1}$  with an average of  $180 \pm 25 \text{ Bq kg}^{-1}$ .  $^{238}\text{U}$  and  $^{232}\text{Th}$  was correlated in sand samples indicating the presence of monazite and zircon rich U and Th respectively. The higher concentration of monazite could be attributed to its significant supply of fine grain sediments from the hinterland areas by the Mahanadi River system and its tributaries (Mohanty et al. 2004a).

The absorbed  $\gamma$  dose rates in air for the Erasama beach region, on the eastern coast of Orissa was found to vary from 650 to 3,150  $\text{nGyh}^{-1}$  with a mean ( $\pm \text{SD}$ )

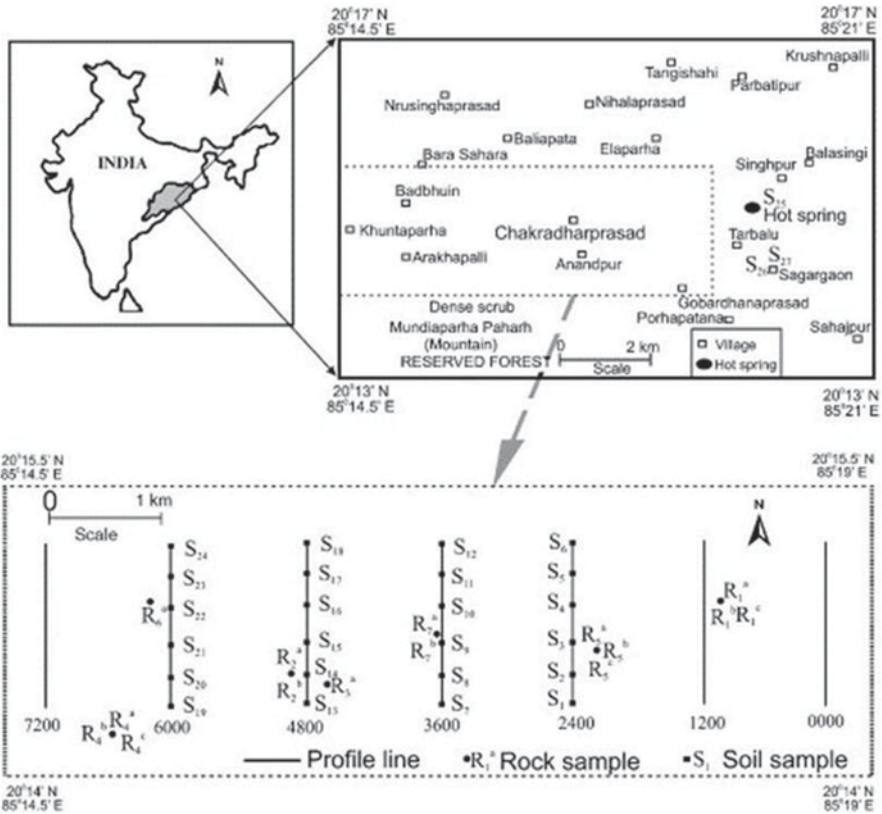


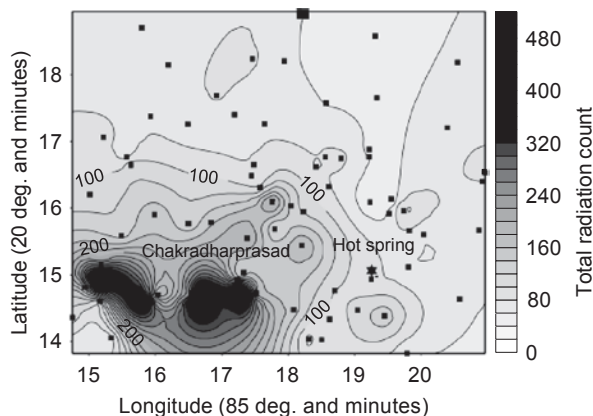
Fig. 6 Survey area and sample locations in Tarbalu region, Orissa (After Baranwal et al. 2006)

value of  $1,925 \pm 718 \text{ nGyh}^{-1}$  and the annual external effective equivalent dose rate of  $2.0 \pm 1.5 \text{ mSv yr}^{-1}$ . Based on the higher levels of natural radioactivity and gamma-absorbed dose rates in air, compared to other monazite rich areas, this region can be considered an HBRA and is comparable to other monazite sand-bearing HBRAs in southern and southwestern coastal regions of India (Mohanty et al. 2004a).

## 2.2 Tarbalu Hot Spring, Orissa, India

Presence of radioactive mineral deposits enhances the background radiations in the area and this helps in the detection of such deposits. However, they also produce heat, called radiogenic heat, which is a source of heat for hot springs. Tarbalu is one such hot spring in the geothermal region of the Eastern Ghats metamorphic province in Orissa, India (Fig. 6). The study area extends from Lat.  $20^{\circ}14' - 20^{\circ}15.5' \text{ N}$ ,

**Fig. 7** Isorad map of the study area (value in total counts per 100 s). *Solid squares* represents data point locations (Taken from Baranwal and Sharma 2005)



and Long.  $85^{\circ}14.5' - 85^{\circ}19'E$ . The study area is characterized by high-grade metamorphic rocks of granulite facies such as khondalite, charnockite, and enderbite, with interlayered mafic horizons (Kundu et al. 2002). It is worth mentioning that deformed granites were found coinciding with high-radioactivity zones, and these high-radioactivity zones are aligned in the east–west direction.

A radiometric reconnaissance survey was carried out in the adjoining geothermal region by Baranwal et al. (2006) using a portable GM counter to identify a relatively high natural background radiation region. Soil and rock samples were collected from these HBRA regions for further measurements in the laboratory to determine the relative concentration of radioactive elements,  $^{238}\text{U}$ ,  $^{232}\text{Th}$ , and  $^{40}\text{K}$ , responsible for high radiation level. Soil and rock sampling locations and the corresponding profiles in the high-radiation area are shown in Fig. 6. The samples were analyzed by  $\gamma$ -ray spectrometry (GRS) using NaI(Tl) and HPGe detector.

## Radiometric Studies

The entire region near the hot spring was surveyed using a portable pulsed GM counter. The contour map over the area is shown in Fig. 7. Soil and rock samples were collected along four profiles (Fig. 6) based on high-radiation areas identified (Fig. 7). The profile-wise detailed radiation survey results are provided in Fig. 5. For detailed measurements, counts were measured at an interval of 25 m along all profiles and profile distance was kept at 1200 m to cover the area of study. The sensor of GM counter was kept approximately at 1 foot above the ground surface to have the appropriate geometry for subsequent sample collection and device was operated for 100 s. From the data obtained in the survey a high background radiation zone was identified (shaded area in Fig. 8) (Baranwal et al. 2006).

Total radiation counts measured over all the profiles are shown as linear plots (Fig. 8a–g) for simplicity and quick correlation among them to identify the high background radiation zones. Soil samples were collected at 200 m intervals from

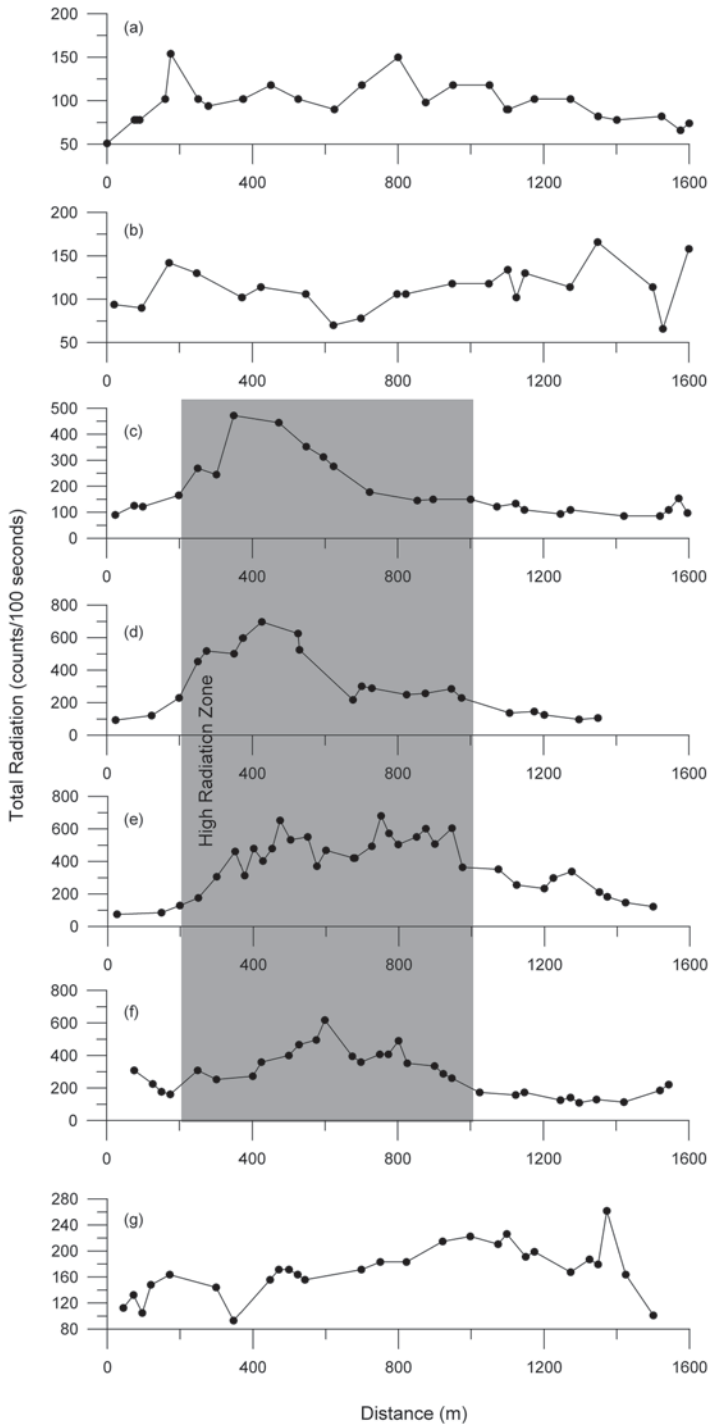


**Fig. 8** Total radiation (counts per 100 s) for different profiles. **a** 0000. **b** 1200. **c** 2400. **d** 3600. **e** 4800. **f** 6000. **g** 7200. *Shaded region* represents high-radiation zones (After Baranwal et al. 2006)

four profiles (2400, 3600, 4800 and 6000) exhibiting the higher radiations. A few rock samples were also collected wherever outcrop was found exposed along these profiles. Subsequently, rock and soil samples were crushed and powdered for gamma ray spectrometry (GRS) analysis and dose rate calculations.

$\gamma$ -ray spectrometric analysis was carried out using NaI(Tl) detector and HPGe detector to estimate the actual concentration of radionuclides. Since radioactive elements emit various energies, high energies were utilized for analysis using a NaI(Tl) detector and low energies using an HPGe detector, respectively. HPGe detectors have better resolution than NaI(Tl) detectors for low energies and so they show sharp peaks for corresponding energies of its decay products, whereas, efficiency of NaI(Tl) detector is higher. The concentration of thorium, equivalent radium, and potassium were estimated. The actual concentration of uranium was also estimated using  $\beta$ - $\gamma$  technique (Eichholz et al. 1953).

Absorbed gamma dose rates were also calculated based on the guidelines of UNSCEAR (1993, 2000). The expression to calculate dose rate is

$$D = (0.692C_{\text{Th}} + 0.462C_{\text{U}} + 0.0417C_{\text{K}}) \text{ nGy/h} \quad (3)$$

where, 0.692 nGy/h is the conversion factor for Th, 0.462 nGy/h is the conversion factor for uranium and 0.0417 nGy/h is the conversion factor for potassium.  $C_{\text{Th}}$ ,  $C_{\text{U}}$ , and  $C_{\text{K}}$  are average activity concentrations (in Bq/kg) of thorium, uranium, and potassium, respectively.

## Results and Discussion

High-radiation zones were identified along four profiles (Fig. 8c–f) with a maximum value of 650 counts/100 s. The width of these zones varies from 200–1,400 m with widest zone along profile 4800. Much of this radiation is due to thorium, since concentration of thorium is very high as compared to uranium and potassium. The maximum concentration of thorium was observed to be 1,194 and 1,066 ppm in sample from profile 3600 and 4800, respectively. Granitic rocks exhibited higher thorium content than other rocks found in the area. Activity concentration of the radionuclides in soil samples also showed high thorium concentration. The presence of thorium was also confirmed by analysis of rock samples using HPGe detector, since the result shows distinct energy peaks corresponding to various isotopes in the decay chain of thorium. The absorbed gamma dose rate in air and external annual dose rate of the high-radiation zone were estimated to be 2431 nGy $^{-1}$  and 2.99 mSvy $^{-1}$ , respectively, which is 10 times greater than outside the high-radiation zones. The high concentration of thorium in the samples also supports the possibility of radiogenic heating to be the source of subsurface heat flow and hence, that of the hot springs (Baranwal et al. 2006).

### 2.3 *Radiometric Study of Coastal, Beach, and the Monazite Placer Deposits*

Beach placer deposits are reported worldwide to be the major source of economically extractable heavy minerals, mostly monazites, zircon, ilmenite, rutile, garnet, sillimanite (Sulekha Rao and Misra 2009). Globally, high-resolution radiometric methods were employed effectively in heavy mineral deposit exploration and associated studies (Grosz 1983; Noakes et al. 1989; de Meijer et al. 1997). Mohanty et al. (2004a, b), Sengupta et al. (2005) and Sulekha Rao et al. (2009) studied the beach deposits at Chhatrapur, Erasama, Gopalpur, and Rushikulya beach on the Orissa coast.

#### **Radiometric Studies**

Samples were collected and subjected to the standard procedure of sample preparation as mentioned earlier. The samples were sealed in plastic vials to attain secular equilibrium. The  $\gamma$ -spectrometric analysis was done using HPGe (EG & G, ORTEC) to determine the activity concentration of the radionuclides. Absorbed  $\gamma$ -dose rate, effective dose rate, radium equivalent activity, and level index were calculated from the activity concentration based on standard equations provided by UNSCEAR and NEA-OECD (Sulekha Rao et al. 2009).

#### **Results and Discussion**

For the Gopalpur samples, the average activity concentrations of  $^{232}\text{Th}$  was  $1,670 \pm 340 \text{ Bq kg}^{-1}$ , for  $^{238}\text{U}$  an average activity of  $200 \pm 40 \text{ Bq kg}^{-1}$  and for  $^{40}\text{K}$  an average activity of  $650 \pm 110 \text{ Bq kg}^{-1}$  was found. For Rushikulya samples, the average activity concentrations of  $^{232}\text{Th}$ ,  $^{238}\text{U}$ , and  $^{40}\text{K}$  was  $990 \pm 250 \text{ Bq kg}^{-1}$ ,  $100 \pm 25 \text{ Bq kg}^{-1}$  and  $775 \pm 100 \text{ Bq kg}^{-1}$ , respectively. For Chhatrapur samples, the average activity concentrations of  $^{232}\text{Th}$ ,  $^{238}\text{U}$ , and  $^{40}\text{K}$  was  $2500 \pm 1850 \text{ Bq kg}^{-1}$ ,  $220 \pm 135 \text{ Bq kg}^{-1}$ , and  $120 \pm 80 \text{ Bq kg}^{-1}$ , respectively (Mohanty et al. 2004b). However, apart from the activity and calculated dose rates the radiometric studies revealed various other significant implications. High radioactivity in the sand dune samples indicated these regions as potential zones for radiogenic minerals. Higher (40–67 times) mean activity than world average of  $^{232}\text{Th}$  suggests predominance of thorium rich monazites (Sulekha Rao et al. 2009). The thorium uranium ratio calculated from the activity also offers valuable insight into the host environment. A higher Th/U concentration ratio suggests enrichment of heavy minerals in the rocks as observed in Gopalpur, Rushikulya beach deposits. The eTh/eU ratio calculated provides information about the geochemical facies, the oxidizing/reducing conditions of the environment. In Gopalpur and Rushikulya beach the average eTh/eU

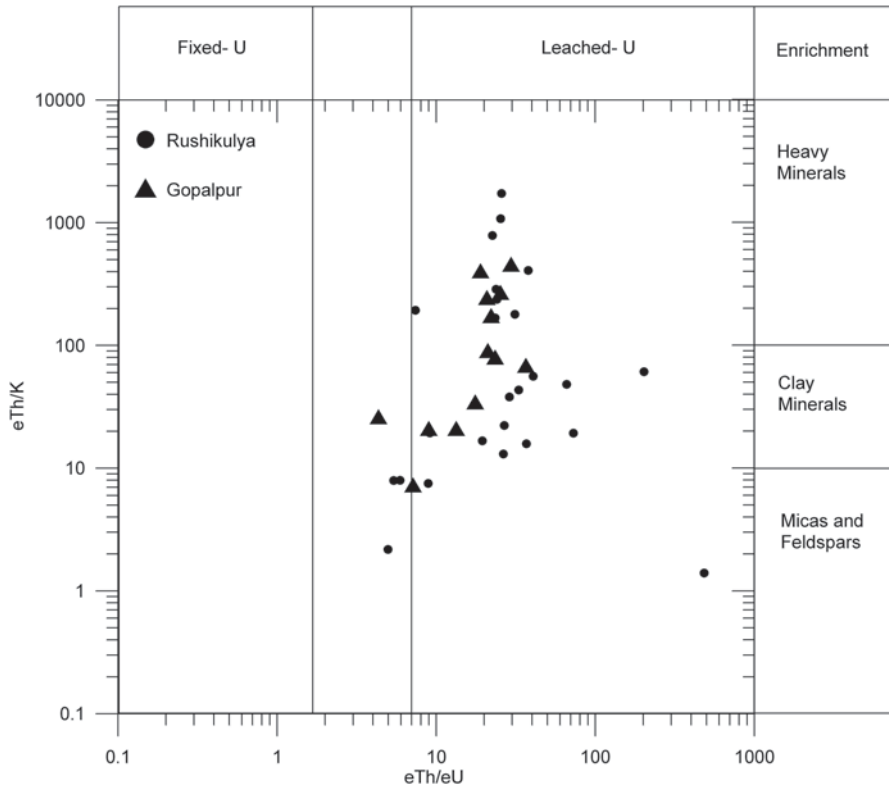


**Fig. 9** Cross plot of  $eTh/eU$  vs.  $eTh/K$  on sand samples of Gopalpur and Rushikulya beach placer deposits, Orissa, India, plotted on the discrimination diagram of Anjos et al. 2006 (After Sulekha Rao et al. 2009)

ratio suggests uranium mobilization through weathering and/or leaching conditions indicating an oxidizing terrestrial environment. The cross plot between  $eTh/eU$  and  $eTh/k$  (fig. 9) showed that majority of Gopalpur falls in heavy mineral field and Rushikulya samples in clay mineral field (Sulekha Rao et al. 2009).

#### 2.4 Radon Migration Study From Uranium Tailings Pond

Uranium tailings are a major source for anthropogenic radon. The tailings are wastes generated from uranium mining and milling activities and are reported to contain  $^{226}Ra$  activity similar to  $^{238}U$  present in the ore before extraction. The contamination from the tailings pond can be through dispersion in air and water (Banerjee 2011). Radon is emitted from the tailings either in form of emanation or exhalation (Sahoo et al. 2010). The study by Sahoo et al. (2010) investigated the seasonal variation of Radon flux over the U tailings pond and generated preliminary data for modelling radon flux from the tailings surface. Figure 10 shows the study area.

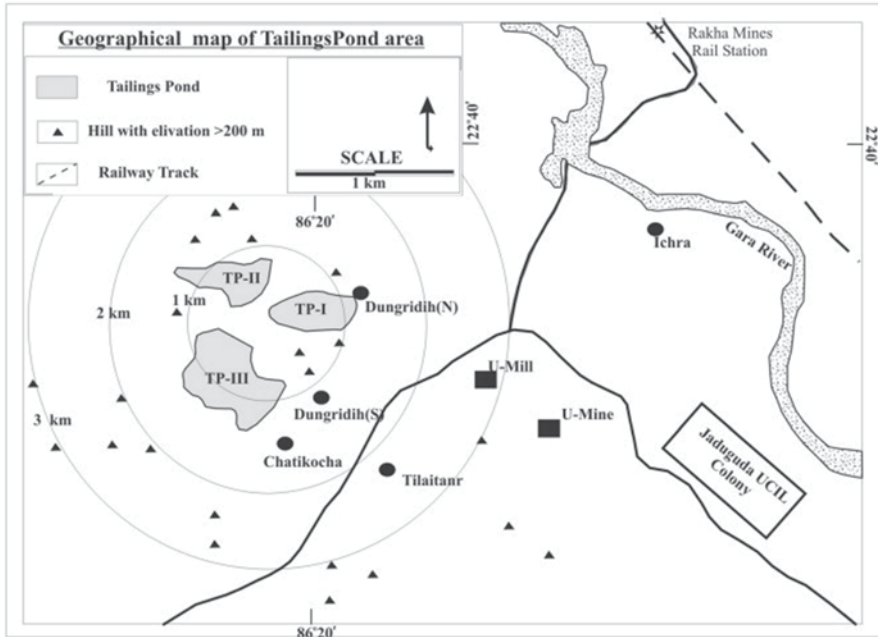


Fig. 10 Geographical map of U tailings pile region at Jaduguda, Jharkhand, India. (After Sahoo et al. 2010)

### Radiometric Studies

Based on the accumulator technique developed by Mayya (2004), in situ radon flux was measured. The accumulator, of 30 cm diameter and 30 cm height, was attached to a continuous radon monitor (AlphaGuard). The set up was installed on the tailings surface and was made air-tight (Fig. 11a). The radon concentrations were recorded at an interval of 10 min for 2–3 h starting from the deployment time considering the saturation state. Equation 4 (Aldenkamp et al. (1992), Sahoo et al. 2010) was used to fit the concentrations data with elapsed time, after necessary corrections:

$$C(t) = \frac{J_s^m A}{V \lambda_e} (1 - e^{-\lambda_e t}) + C_0 e^{-\lambda_e t} \tag{4}$$

Where  $J_s^m$  is the radon flux from tailings surface ( $Bq\ m^{-2}\ s^{-1}$ ),  $V$  is the accumulator volume ( $m^3$ ),  $\lambda_e$  denotes the effective decay constant ( $s^{-1}$ ) of radon for the given set up and is given by sum of radon decay constant, leakage rates (if any) and back-diffusion rate for the set up.  $A$  is the soil surface area under the accumulator ( $m^2$ ) and  $C_0$  is initial radon concentration inside the accumulator at  $t=0$ .

Theoretical radon fluxes were calculated from the in-situ radon emanation values using UNSCEAR 2000 formula (Sahoo et al. 2010):

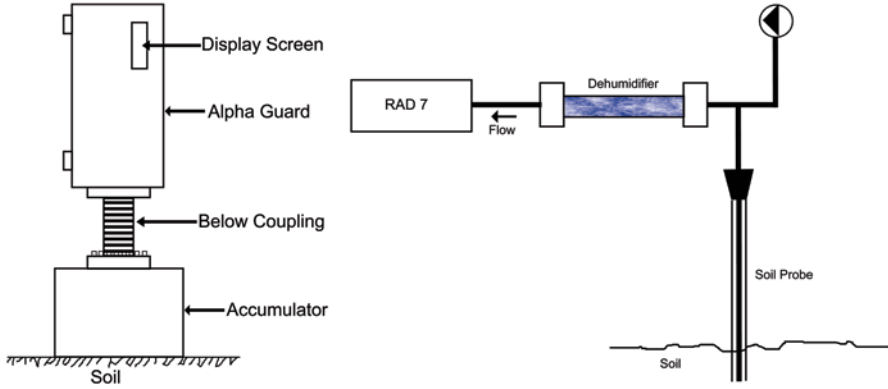


**Fig. 11 a** Experimental setup for in-situ radon flux measurement (After Sahoo et al. 2010). **b** Experimental setup for the measurement of radon concentration at different depth in U tailings (After Sahoo et al. 2010)

$$J_s^e = \lambda l_s Q_{Ra} \rho_b f \quad (5)$$

Where the soil radium content ( $\text{Bq kg}^{-1}$ ) is given by  $Q_{Ra}$ ,  $\rho_b$  denotes the soil bulk density ( $\text{kg m}^{-3}$ ),  $f$  is radon emanation factor measured in situ,  $l_s$  (m) is the radon diffusion length in the tailings and the decay constant for  $^{222}\text{Rn}$  ( $\text{s}^{-1}$ ) is given by  $\lambda$ .

Tailings parameters were calculated from samples collected by introducing a 1000 cc stainless steel cylinder into the tailings. The samples were processed followed by oven drying at  $110^\circ\text{C}$  to attain constant weight and sealed in 300 cc plastic containers for gamma spectrometric analysis.  $^{226}\text{Ra}$  in the tailings ( $Q$ ) (after Shukla et al. 2001, c. i. in Sahoo et al. 2010), radon mass exhalation rate, radon emanation factor in-situ ( $f$ ) and in dry conditions ( $f_0$ ) (after Sahoo et al. 2007) was measured. Soil porosity ( $\epsilon$ ) and  $S$  was calculated using the relations given by Rogers and Nielson (1991) in Sahoo et al. (2010) (Eq. 6):

$$(\epsilon) = [1 - \rho_b / \rho_g] \quad (6)$$

(where  $\rho_a$  is the average specific gravity of soil ( $2700 \text{ kg m}^{-3}$ ) and  $\rho_b$  is the dry bulk density ( $\text{kg m}^{-3}$ ) of tailings) and  $100S = \rho_b M_w / \rho_w \epsilon$  where  $M_w$  is soil water content (dry weight percent) and  $\rho_w$  is the density of water ( $\text{kg m}^{-3}$ ), respectively. The temperature at 10 cm depth from tailings surface was measured in situ using a temperature sensor. Depth profile of radon concentration in the U tailings pile was used to estimate the in situ radon diffusion lengths ( $l_s$ ). Online radon monitor with silicon alpha detector (RAD 7, Durrige Company Inc, Bedford) was used to measure radon concentrations in the tailings pond. Readings were taken by air sample collection at the rate of  $0.5 \text{ L min}^{-1}$  through a probe (Fig. 11b) at an interval of 20 cm up to a depth of 120 cm. The radon concentration vs. soil depth was plotted and fitted to the concentration depth profile using equation (Eq. 7) (Nazaroff and Nero 1988 c.i. Sahoo et al. 2010).

$$C(z) = C_{\infty} (1 - \exp(-z / l_s)) \quad (7)$$

where,  $C(z)$  is the  $^{222}\text{Rn}$  concentration ( $\text{Bq m}^{-3}$ ) at a depth  $z$  (cm),  $C_{\infty}$  is the  $^{222}\text{Rn}$  concentration at deeper depth ( $\text{Bq m}^{-3}$ ) and  $l_s$  (cm) is the diffusion length of  $^{222}\text{Rn}$  in soil.

## Results and Discussion

The radon fluxes at different locations of U tailings pile at Jaduguda, India showed a weak seasonal variation (Sahoo et al. 2010). The mean values of radon fluxes obtained were  $3.74 \pm 2.18$ ,  $3.27 \pm 1.82$ , and  $4.24 \pm 1.83$   $\text{Bq m}^{-2} \text{ s}^{-1}$  in winter, summer, and rainy seasons, respectively (Sahoo et al. 2010). From this data, the radon source term contributed from this area was estimated as  $8.1 \pm 10^{13}$   $\text{Bq y}^{-1}$  (Sahoo et al. 2010). A good linear correlation was observed between  $^{226}\text{Ra}$  contents and seasonal averaged radon fluxes in tailings (Sahoo et al. 2010). The slope of value  $(8.3 \pm 0.4) \times 10^{-4}$   $\text{kg m}^{-2} \text{ s}^{-1}$  was used as a conversion factor for the quick estimation of radon flux ( $\text{Bq m}^{-2} \text{ s}^{-1}$ ) using  $^{226}\text{Ra}$  ( $\text{Bq kg}^{-1}$ ) in U tailings or vice versa (Sahoo et al. 2010).

### 2.5 Radiometric Studies for Shallow Uranium Deposits

In nature the ambient geological and geochemical conditions (oxidation, reduction, Eh, pH, etc.) determines the concentration of radionuclide in minerals and rocks. A lithological unit, primary and unaltered, in a geological region can be characterized by a certain range of radioactivity (Savosin and Sinitsyn 1965). However, subjected to successive geological episodes there can be considerable changes in the radioactivity of the same. The radionuclides and the decay products of some of them emit highly energetic penetrating radiations like  $\gamma$ -rays. When analyzed, different  $\gamma$ -rays with different energies gives out a spectrum composed of various photo peaks. This  $\gamma$ -ray spectrum can be used to obtain the activity concentration of the respective radionuclides present in the source material. In a similar study by Mittal et al. (2013), the nature of uranium mineralization in SPSZ as well as the efficacy of this zone as an economic uranium prospect was investigated. The study area lies around SPSZ in Purulia district of West Bengal, India. The shear zone is an arc type curvilinear tectonic zone extending from Tamar in the west to Khatra in the east with a strike extension of 120–150 km and an average width of  $\sim 4$ –5 km. To the north of it lies the Chhotanagpur Granite Gneissic Complex (CGGC) and in south it is bounded by the Singhbhum Group.

The area is mainly made up of meta-sedimentary rock suites (Bhattacharya et al. 1991) and the major rock types include Tuffaceous-phyllite, Schist, Quartzite, Pyroxenite, Carbonatite, Quartz-magnetite-apatite, Tourmalinite, Quartz breccias, Alkali granites, Alkaline ultramafics (Chakrabarty et al. 2009). Moderate-to-steep dip

foliations, ductile to brittle-ductile characters are also found in the rocks comprising the study area. Initial survey was done using portable GM counter for identifying the sampling locations. Samples were then collected from those sites exhibiting higher radioactivity than background, for  $\gamma$ -ray spectrometric study. All the samples (soil and rock) were crushed, dried, and cooled to the room temperature, and followed by sieving to a particular size, coning, and quartering in order to achieve a homogeneous representation of the bulk samples. Known amounts of the soil and rock samples were sealed in plastic vials, labelled, and kept for a minimum duration of 40 days to attain the secular equilibrium. Subsequently, the samples were then subjected to  $\gamma$ -ray spectrometric analysis for  $^{238}\text{U}$ ,  $^{232}\text{Th}$ , and  $^{40}\text{K}$  measurements using HPGe  $\gamma$ -ray spectrometry system (EG & G, ORTEC) with 50% relative efficiency.

The activity concentration of  $^{238}\text{U}$  in the samples ranges from  $61.5 \pm 2.3$  to  $276.7 \pm 2.6$  Bq/kg,  $^{232}\text{Th}$  ranges from  $66.3 \pm 18.9$  to  $246.9 \pm 3.2$  Bq/kg, and  $^{40}\text{K}$  ranges from  $2354.2 \pm 3.8$  to  $6329.7 \pm 15.8$  Bq/kg, respectively. Uranium content showed a decreasing trend towards the periphery and highest concentration at the central part of the shear zone. It is important to note that the central part of the zone represents a zone of intense shearing; this implies that shearing has an active control on distribution of radionuclides. The uranium activity also showed a similar trend of decrement away from the central part of shear zone. This is because the local soil is the weathered product of rocks and the distribution of radioactive elements is significantly affected by the geological processes like solution activity, weathering, erosion, leaching, etc. (Åkerblom and Mellander 1997). Therefore, soil samples showed a higher radiation level compared to the rocks. The U:Th ratio indicated an enrichment of Uranium in the central part that decreased radially outward. As compared to average Indian values, the concentration of uranium is found higher in the study area. This suggests the possibility of shallow uranium deposits in the area along the shear zone.

## References

- Åkerblom G, Mellander H (1997) Geology and radon. In: Durrani SA, Ilic' R (eds) Radon measurements by etched track detectors: applications to radiation protection, earth sciences and the environment. World Scientific press, Singapore, pp 21–49
- Aldenkamp FJ, de Meijer RJ, Put LW, Stoop P, (1992) An assessment of in-situ radon exhalation measurements and the relation between free and bound exhalation rate, Radiation Protection Dosimetry 45:449–453
- Banerjee KS (2011) Measurement of source term for environmental radioactivity and study of geologic control on radon release in a uranium mineralized zone, Jharkhand, India. Unpublished doctoral dissertation thesis, Indian Institute of Technology Kharagpur, Kharagpur, India, 61
- Baranwal VC, Sharma SP (2005) Integrated geophysical studies in the East-Indian geothermal province. Pure Appl Geophys 163:209–227
- Baranwal VC, Sharma SP, Sengupta D, Sandilya MK, Bhaumik BK, Guin R, Saha SK (2006) A new high background radiation area in the geothermal region of Eastern Ghats Mobile Belt (EGMB) of Orissa, India. Radiat Meas 41:602–610

- Bhattacharya C, Chakraborty A, Banerjee PK (1991) Petrology-geochemistry of apatite-magnetite amphibolites and their role in phosphate mineralisation along the southern shear zone, Puruliya District, West Bengal. *Indian J Earth Sci* 18:94–109
- Chakrabarty A, Sen AK, Ghosh TK (2009) Amphibole—a key indicator mineral for petrogenesis of the Puruliacarbonatite, West Bengal, India. *Mineral Petrol* 95(1–2):105–112
- Cullen TL (1977) A review of Brazilian investigations in areas of high natural radioactivity, Part I: radiometric and dosimetric studies. In: Cullen TL, Penna Franca E (eds) *Proceedings of international symposium on areas of high natural radioactivity, 1975*. Academia Brasileria De Ciencias, Rio de Janeiro, pp 49–64
- de Meijer RJ, Stapel C, Jones DG, Roberts PD, Rozendaal A, Macdonald WG (1997) Improved and new uses of natural radioactivity in mineral exploration and processing. *Explor Min Geol* 6:105–117
- Eichholz GG, Hilborn JW, McMahon C (1953) The determination of uranium and thorium in ores. *Can J Phys* 31:613–628
- Firestone RB, Shirley VS (1998) *Table of isotopes*, 8th edn. Wiley, New York
- Ghiassi-nejad M, Mortazavi SMJ, Cameron JR, Niroomand-rad A, Karam PA (2002) Very high background radiation areas of Ramsar, Iran: preliminary biological studies. *Health Phys* 82:87–93
- Grigorescu EL, Razdolescu AC, Sahagia M, Luca A, Ivan C, Tanase G (2002) Standardization of  $^{152}\text{Eu}$ . *Appl Radiat Isot* 56:435–439
- Grosz AE (1983) Applications of total count aeroradiometric maps to the exploration for heavy-mineral deposits in the coastal plain of Virginia. *US Geological Survey Prof. Paper* 1263
- Khandaker MU (2011) High purity germanium detector in gamma-ray spectrometry. *Int J Fundam Phys Sci* 1(2):42–46
- Kundu N, Panigrahi MK, Sharma SP, Tripathy S (2002) Delineation of fluoride contaminated groundwater around a hot spring in Nayagarh, Orissa, India using geochemical and resistivity studies. *Environ Geol* 43:228–235
- Mayya YS (2004) Theory of radon flux into accumulators placed at the soil-atmosphere interface. *Radiat Dosim* 111:305–318
- Mittal S, Guin R, Sharma SP, Sengupta D (2013) Estimation of  $^{238}\text{U}$ ,  $^{232}\text{Th}$  and  $^{40}\text{K}$  Concentrations in Rock and Soil Samples Around South Purulia Shear Zone, India. *International Journal of Low Radiation* 9:110–118
- Mohanty AK, Sengupta D, Das SK, Vijayan V, Saha SK (2004a) Natural radioactivity in the newly discovered high background radiation area on the eastern coast of Orissa, India. *Radiat Meas* 38:153–165
- Mohanty AK, Sengupta D, Das SK, Saha SK, Van KV (2004b) Natural radioactivity and radiation exposure in the high background area at Chhatrapur beach placer deposit of Orissa, India, *J. Environ. Radioact* 75:15–33
- Nazaroff W W and Nero Jr. A V (1988). In: John Wileyand Sons Inc. (Ed.), *Radon and its decay products in indoor air*, pp 57–112, New York.
- Noakes JE, Harding JL, Staehle CM (1989) Survey of nuclear methods applied to marine mineral exploration. *Mar Min* 8:215–244
- Paul AC, Pillai PMB, Haridasan P, Radhakrishnan S, Krishnamony S (1998) Population exposure to airborne thorium at the high natural radiation areas in India. *J Environ Radioactiv* 40:251–259
- Rogers VC, Nielson KK (1991) Multiphase radon generation and transport in porous materials. *Health Phys* 60:807
- Sahoo BK, Nathwani D, Eappen KP, Ramachandran TV, Gaware JJ, Mayya YS (2007) Estimation of radon emanation factor in Indian building materials. *Radiat Meas* 42:1422–1425
- Sahoo BK, Mayya YS, Sapra BK, Gaware JJ, Banerjee KS, Kushwaha HS (2010) Radon exhalation studies in an Indian uranium tailings pile. *Radiat Meas* 45:237–241
- Savosin SI, Sinitsyn VI (1965) Application of methods of nuclear geophysics in ore prospecting, exploration, and development. Translated from *Atomnaya ~nergiya*, Vol. 18, 1, pp 81–84

- Sengupta D, Mohanty A K, Das S K and Saha S K (2005) Natural radioactivity in the high background radiation area at Erasama beach placer deposit of Orissa, India, International Congress Series, 1276, pp. 210–211
- Shukla VK, Sartendel SJ, Ramachandran TV (2001) Natural radioactivity level in soil from high background radiation areas of Kerala. *Radiat Prot Environ* 24:437–439
- Smith HA Jr, Lucas M (1991) Gamma-ray detectors. In: Reilly D, Ensslin N, Smith Hastings Jr (eds) *Passive nondestructive assay of nuclear materials*. NuREG/cR-5550, LA-UR-90-732., pp 43–64. <http://www.lanl.gov/orgs/n/n1/panda/00326398.pdf>. Accessed 24 Sept 2013
- Sohrabi M (1993) Recent radiological studies of high level natural radiation areas of Ramsar. In: *Proceedings of the International Conference on High Levels of Natural Radiation Areas, 1990*, Ramsar, Iran. IAEA Publication Series, IAEA, Vienna
- Sengupta D, Mohanty AK, Das SK, Saha SK (2005) Natural radioactivity in the high background radiation area at Erasama beach placer deposit of Orissa, India, International Congress Series, 1276, pp 210–211
- Sulekha Rao N, Misra S (2009) Sources of Monazite Sand in Southern Orissa Beach Placer, Eastern India, *Journal of Geological Society of India*, Vol. 74, September 2009, pp 357–362
- Sunta CM, David M, Abani MC, Basu AS, Nambi KSV (1982) Analysis of dosimetry data of high natural radioactivity areas of southwest coast of India. In: Vohra KG et al (ed) *The natural radiation environment*. Wiley Eastern Limited, India, pp 35–42
- UNSCEAR (1993) *Sources and effects of ionizing radiation*. New York, United Nations Scientific Committee on the Effect of Atomic Radiation
- UNSCEAR (2000) *Sources and effects of ionizing radiation*. New York, United Nations Scientific Committee on the Effect of Atomic Radiation
- Wei L, Sugahara T (2000) An introductory overview of the epidemiological study on the population at the high background radiation areas in Yangjiang, China. *J Radiat Res* 41(Suppl):1–7
- Wei L, Zha Y, Tao Z, He W, Chen D, Yuan Y (1993) Epidemiological investigation in high background radiation areas in Yangjiang, China. In: *Proceedings of the international conference on high levels of natural radiation areas, Ramsar, Iran, 1990*. IAEA Publication Series, IAEA, Vienna, pp 523–547